A Letters Journal Exploring the Frontiers of Physics

OFFPRINT

Dynamic jamming fronts

S. R. Waitukaitis, L. K. Roth, V. Vitelli and H. M. Jaeger

EPL, **102** (2013) 44001

Please visit the new website
www.epljournal.org

epl

A LETTERS JOURNAL EXPLORING THE FRONTIERS OF PHYSICS

AN INVITATION TO SUBMIT YOUR WORK

www.epljournal.org

The Editorial Board invites you to submit your letters to EPL

EPL is a leading international journal publishing original, high-quality Letters in all areas of physics, ranging from condensed matter topics and interdisciplinary research to astrophysics, geophysics, plasma and fusion sciences, including those with application potential.

The high profile of the journal combined with the excellent scientific quality of the articles continue to ensure EPL is an essential resource for its worldwide audience. EPL offers authors global visibility and a great opportunity to share their work with others across the whole of the physics community.

Run by active scientists, for scientists

EPL is reviewed by scientists for scientists, to serve and support the international scientific community. The Editorial Board is a team of active research scientists with an expert understanding of the needs of both authors and researchers.

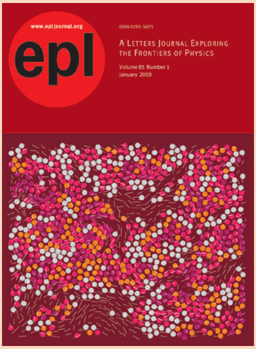

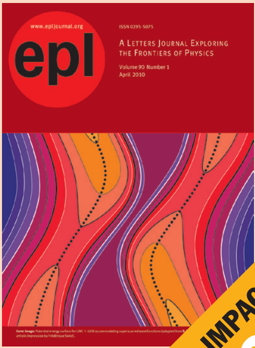

IMPACT FACTOR 2.753*

* As ranked by ISI 2010

www.epljournal.org

IMPACT FACTOR
2.753*
* As listed in the ISI® 2010 Science Citation Index Journal Citation Reports

OVER
500 000
full text downloads in 2010

30 DAYS
average receipt to online publication in 2010

16 961
citations in 2010
37% increase from 2007

"We've had a very positive experience with EPL, and not only on this occasion. The fact that one can identify an appropriate editor, and the editor is an active scientist in the field, makes a huge difference."

Dr. Ivar Martinv
Los Alamos National Laboratory, USA

Six good reasons to publish with EPL

We want to work with you to help gain recognition for your high-quality work through worldwide visibility and high citations.

1. **Quality** – The 40+ Co-Editors, who are experts in their fields, oversee the entire peer-review process, from selection of the referees to making all final acceptance decisions
2. **Impact Factor** – The 2010 Impact Factor is 2.753; your work will be in the right place to be cited by your peers
3. **Speed of processing** – We aim to provide you with a quick and efficient service; the median time from acceptance to online publication is 30 days
4. **High visibility** – All articles are free to read for 30 days from online publication date
5. **International reach** – Over 2,000 institutions have access to EPL, enabling your work to be read by your peers in 100 countries
6. **Open Access** – Articles are offered open access for a one-off author payment

Details on preparing, submitting and tracking the progress of your manuscript from submission to acceptance are available on the EPL submission website **www.epletters.net**.

If you would like further information about our author service or EPL in general, please visit **www.epljournal.org** or e-mail us at **info@epljournal.org**.

EPL is published in partnership with:

European Physical Society | Società Italiana di Fisica | EDP Sciences | IOP Publishing

epl

A LETTERS JOURNAL EXPLORING THE FRONTIERS OF PHYSICS

EPL Compilation Index

www.epljournal.org

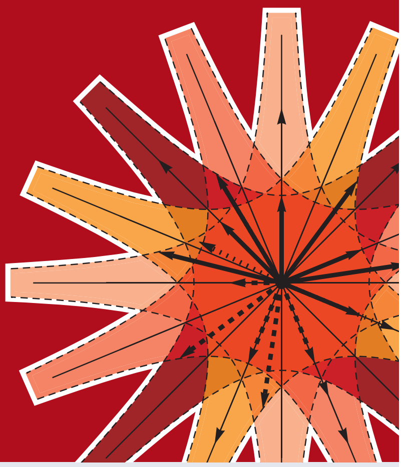

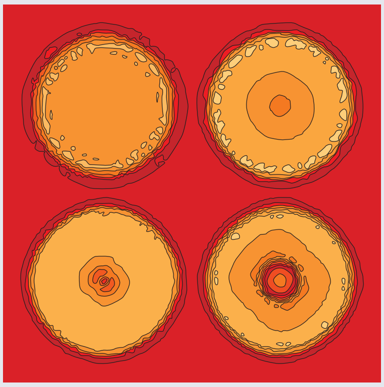

Biaxial strain on lens-shaped quantum rings of different inner radii, adapted from **Zhang *et al*** 2008 EPL **83** 67004.

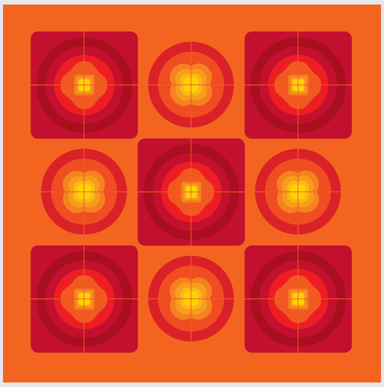

Artistic impression of electrostatic particle–particle interactions in dielectrophoresis, adapted from **N Aubry and P Singh** 2006 *EPL* **74** 623.

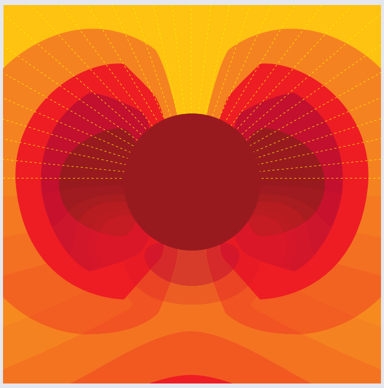

Artistic impression of velocity and normal stress profiles around a sphere that moves through a polymer solution, adapted from **R Tuinier, J K G Dhont and T-H Fan** 2006 *EPL* **75** 929.

Visit the EPL website to read the latest articles published in cutting-edge fields of research from across the whole of physics.

Each compilation is led by its own Co-Editor, who is a leading scientist in that field, and who is responsible for overseeing the review process, selecting referees and making publication decisions for every manuscript.

- Graphene
- Liquid Crystals
- High Transition Temperature Superconductors
- Quantum Information Processing & Communication
- Biological & Soft Matter Physics
- Atomic, Molecular & Optical Physics
- Bose–Einstein Condensates & Ultracold Gases
- Metamaterials, Nanostructures & Magnetic Materials
- Mathematical Methods
- Physics of Gases, Plasmas & Electric Fields
- High Energy Nuclear Physics

If you are working on research in any of these areas, the Co-Editors would be delighted to receive your submission. Articles should be submitted via the automated manuscript system at **www.epletters.net**

If you would like further information about our author service or EPL in general, please visit **www.epljournal.org** or e-mail us at **info@epljournal.org**

EPS Società Italiana di Fisica EDP SCIENCES **IOP** Publishing

Image: Ornamental multiplication of space-time figures of temperature transformation rules (adapted from T. S. Bíró and P. Ván 2010 *EPL* **89** 30001; artistic impression by Frédérique Swist).

A Letters Journal Exploring the Frontiers of Physics

May 2013

EPL, **102** (2013) 44001 www.epljournal.org
doi: 10.1209/0295-5075/102/44001

Dynamic jamming fronts

S. R. Waitukaitis[1], L. K. Roth[2], V. Vitelli[3] and H. M. Jaeger[1]

[1] *Department of Physics and James Franck Institute at the University of Chicago - Chicago, IL 60637, USA*
[2] *Department of Physics, St. Olaf College - Northfield, MN 55057, USA*
[3] *Instituut-Lorentz for Theoretical Physics, Leiden University - Leiden NL 2333 CA, The Netherlands, EU*

received 7 March 2013; accepted in final form 30 April 2013
published online 24 May 2013

PACS 45.70.Cc – Granular systems: Static sandpiles; granular compaction
PACS 83.80.Fg – Granular solids
PACS 05.45.-a – Nonlinear dynamics and chaos

Abstract – We describe a model experiment for dynamic jamming: a two-dimensional collection of initially unjammed disks that are forced into the jammed state by uniaxial compression via a rake. This leads to a stable densification front that travels ahead of the rake, leaving regions behind it jammed. Using disk conservation in conjunction with an upper limit to the packing fraction at jamming onset, we predict the front speed as a function of packing fraction and rake speed. However, we find that the jamming front has a finite width, a feature that cannot be explained by disk conservation alone. This width appears to diverge on approach to jamming, which suggests that it may be related to growing lengthscales encountered in other jamming studies.

editor's choice Copyright © EPLA, 2013

Introduction. – The jamming transition has been studied extensively in experiments and simulations [1–9]. Most studies have focused on the time-independent, bulk characteristics of the jammed state at fixed, uniform packing fraction. However, there are dynamic features related to jamming when the packing fraction is not uniform in space or time. In such systems, traveling jamming fronts delineate between jammed and unjammed regions. In dry granular systems, for example, the stop (start) of flow from a hopper leads to jamming (unjamming) fronts that shoot away from the orifice and define the boundary between flowing and unflowing regions [10,11]. In suspensions, jamming fronts develop when sedimenting particles rain toward a fixed boundary [12] or, in the inverse situation, when a moving boundary forces particles together during surface impact [13].

Here we present an experimental study of a model system to investigate dynamic jamming. The system consists of initially unjammed, binary-sized disks sitting on a plane that are forced toward jamming by uniaxial compression via a rake. Precisely tracking all disks and calculating the instantaneous position, velocity, and packing fraction allows us to characterize the jamming front as it solidifies the system. We determine the front speed by simply assuming that there is an effective upper limit to the densification corresponding to the jamming threshold ϕ_J and that disks are conserved. Surprisingly, however, we find that the fronts have characteristic widths that depend strongly on packing fraction.

Setup. – Images from the experiment are shown in fig. 1. Laser-cut, black acrylic disks are randomly arranged at an initial packing fraction ϕ_0 on an acrylic tray that is backlit from below and recorded from above with a video camera. The disks are cut to diameters $d_l = 1.34\times10^{-2}$ m and $d_s = 9.30\times10^{-3}$ m (*i.e.* $d_l/d_s \approx \sqrt{2}$) and are present in equal number $N_l = N_s$ in order to prevent crystallization [14–18]. The disks are then pushed from the left with a rake connected to a linear actuator that extends at constant velocity v_r. As can be seen from the images in fig. 1, this leads to the formation of a stable densification front that travels ahead of the rake. Behind this front, the grains move with the velocity of the rake and are left in a jammed state with final packing fraction ϕ_J (for full evolution, see supplementary movie bw_movie.mov).

We analyze the videos by first binarizing and watershedding the images in ImageJ [19] in order to separate disks in close proximity. We determine the disk positions by locating all of the unique black domains (excluding the rake/actuator) within each image and calculating their centers of mass. Individual disk trajectories are acquired with the IDL tracking code developed by Crocker and Grier [20]. From these, we calculate the instantaneous disk velocities by subtracting disk positions between frames

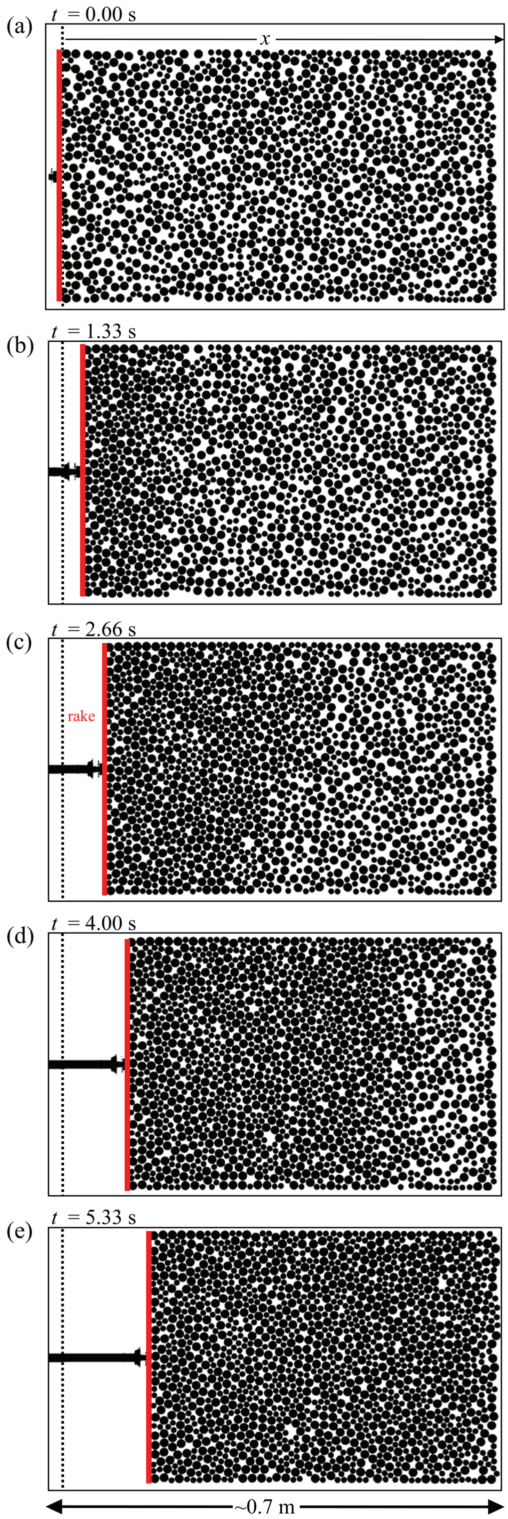

Fig. 1: (Color online) Dynamic jamming experiment. Acrylic, binary disks ($d_l = 1.34 \times 10^{-2}$ m, $d_s = 9.30 \times 10^{-3}$ m, and $h = 9.80 \times 10^{-3}$ m) sit on an acrylic tray ($\sim 0.70\,\mathrm{m} \times 0.38\,\mathrm{m}$). The initial configuration is compressed from the left by a rake (red line) with constant velocity v_r. This creates a stable jamming front that travels ahead of the rake. Images correspond to $\phi_0 = 0.611 \pm 0.003$, rake velocity $v_r = 2.50 \times 10^{-2}$ m/s at times $t = 0.00$ s (a), 1.33 s (b), 2.66 s (c), 4.00 s (d), and 5.33 s (e). For full evolution, see supplementary movie `bw_movie.mov`.

and multiplying by the frame rate (usually ∼10 frames per second). We use the Voronoi tessellation (obtained with Voro++ [21]) to calculate the local, instantaneous packing fraction of each disk (defined as the disk's area divided by the area of its Voronoi cell). In order to extract velocity and packing fraction profiles, we reduce the problem to one dimension and define the coarse-grained velocity field $V(x,t)$ and packing fraction $\phi(x,t)$ by binning the individual disk measurements at a given t along x (binsize $2d_l$) and calculating the bin averages. The variability of in ϕ_0 along these bins is ∼0.01.

Results. – Figure 2 shows a snapshot of an initially uncompacted system (as in the left of the images) a short while after the rake has begun to move. By rendering images of the disks colored by their instantaneous velocity (fig. 2(a)) and packing fraction (fig. 2(b)), we are able to see the microscopic details of front formation. While disks near to the rake generally move with velocity v_r and disks far ahead are stationary, we find velocities over the entire range $[0,\ v_r]$ in the transition region between these extremes. In the same region, one sees that the velocities are not constant along the transverse direction, but instead create finger-like chains of particles that give roughness to the front. When we plot the coarse-grained velocity V *vs.* x (fig. 2(c)), however, these rough protrusions average into to a smooth profile with a soft transition from the rake velocity $V = v_r$ behind the front to $V = 0$ beyond the front. We find empirically that the these profiles are generally well approximated by the equation

$$V(x) = \frac{v_r}{1 + e^{(x - x_f)/\Delta_f}}, \tag{1}$$

where x_f is the location of the center of the front and Δ_f is the width. We see similar profiles for $\phi(x)$ (fig. 2(d)), which can be fit by the similar equation $\phi(x) = \phi_0(1 - 1/(1 + e^{(x - x_f)})) + \phi_J$.

Fitting $V(x)$ to eq. (1) allows us to extract measurements of the front position x_f and width Δ_f for each time t of the experiment. In fig. 3(a), we plot x_f *vs.* t for several different values of ϕ_0 at a rake speed $v_r = 1.00 \times 10^{-2}$ m/s. As the plot shows, the fronts move at constant velocities, which we can measure by fitting to $x_f = v_f t$. Plotting v_f/v_r *vs.* ϕ_0 shows that the front speed appears to diverge as the packing fraction is increased.

This kind of behavior arises from the requirement of disk conservation in combination with the fact that the disks cannot easily be compressed beyond jamming. To see how this works, we start with the conservation equation

$$\phi_t + (V\phi)_x = 0, \tag{2}$$

where the subscripts t and x indicate time and space differentiation, respectively. As is often done [22], we assume an *ad hoc* constitutive equation for ϕ and V, in this case the simple linear relationship

$$\frac{\phi - \phi_0}{\phi_J - \phi_0} = \frac{V}{v_r} \equiv U, \tag{3}$$

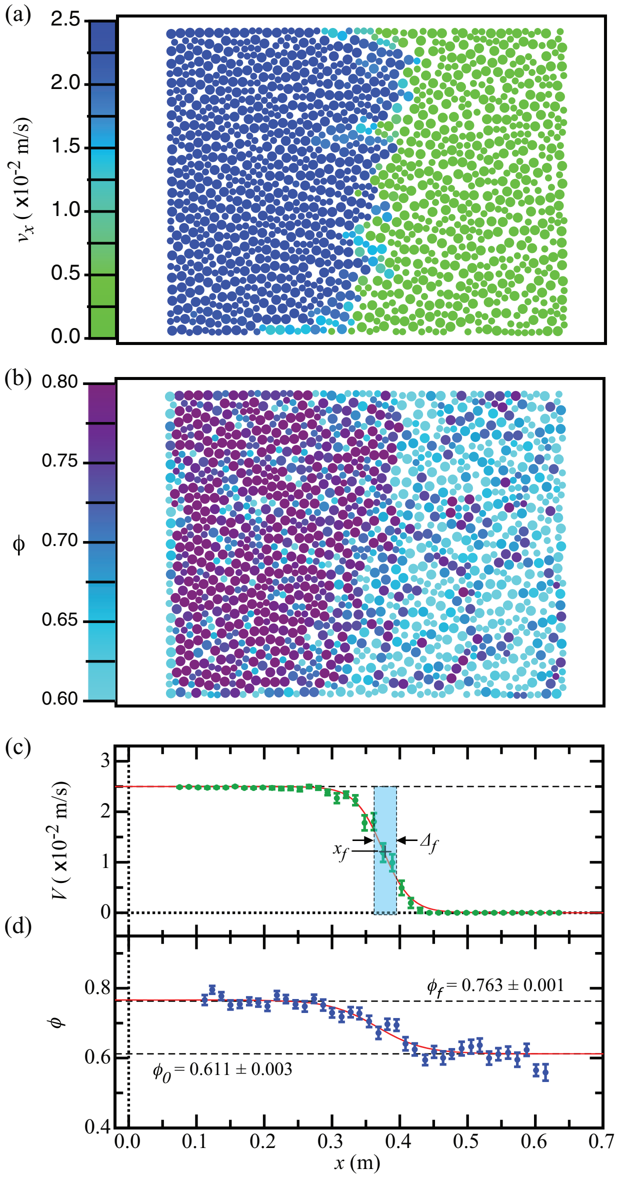

Fig. 2: (Color online) Snapshot of a jamming front. (a) Rendering of disks colored by instantaneous velocity after $t = 4.00$ s in experiment with $\phi_0 = 0.611 \pm 0.003$ and rake velocity $v_r = 2.50 \times 10^{-2}$ m/s. (b) Same as (a) but with disks colored by packing fraction. (c) Profile of the coarse-grained velocity V *vs.* x at same time. The red curve is a fit to eq. (1), from which we extract the front position x_f and width Δ_f (indicated in figure). (d) Profile of the coarse-grained packing fraction ϕ *vs.* x. Error bars in (c) and (d) are the standard deviation of the mean for each x-bin.

where the dimensionless variable U scales between 0 and 1 (we confirmed this is a very good approximation to our data). This form effectively assumes that if the disks are at ϕ_J, they must also be moving at speed v_r, which is reasonable given that the step-like increase of the bulk modulus at jamming [5,9,23] will tend to prevent further compaction and cause disks to move rigidly with the rake. Finally, combining eqs. (2) and (3) results in the Riemann formulation [24] of the inviscid Burgers equation,

$$U_t + \left(U v_r \left(U + \frac{\phi_0}{\phi_J - \phi_0} \right) \right)_x = 0 \qquad (4)$$

whose solutions are of the form $U = U(x - v_f t)$ (note that eq. (1) is a solution assuming $x_f = v_f t$). Using the appropriate boundary conditions for this system, one arrives at the Rankine-Hugoniot condition [24] for the front speed,

$$v_f = v_r \left(1 + \frac{\phi_0}{\phi_J - \phi_0} \right). \qquad (5)$$

The proportionality between v_f and v_r is markedly different from the behavior of systems above jamming, where one encounters shock speeds that are either independent of the driving speed (weak shocks) or scale like $v_r^{1/5}$ (strong shocks) [25,26]. Both above and below jamming, however, the distance to ϕ_J plays a critical role in determining the front speed.

Fitting the data of fig. 3(b) to eq. (5) yields $\phi_J = 0.781 \pm 0.001$. It is clear from the fit, however, that there is a discrepancy at higher values of ϕ_0 as the fitted curve falls to the left of the data. As we are able to measure the final packing fraction for each experiment, we see that this actually arises because there is a trend such that higher ϕ_0 have higher ϕ_J (inset to fig. 3(c)). This variability may arise because of finite system size [5], but could also arise in part from the increased pressure at the front interface at higher v_r. Nonetheless, we achieve better agreement if we use the values of ϕ_J measured from each experiment individually. Doing so in conjunction with eq. (5) accurately describes the front speed over nearly 2 decades in $\phi_J - \phi_0$ (note that the dashed line in fig. 3(c) is a prediction with no fit parameters). The range of values we find for ϕ_J ($\sim$0.76–0.79) is consistent with the results of recent simulations of frictional disks with identical size and number ratios [14,15].

While disk conservation seems like the most natural starting point for modeling this system, it is incapable of predicting the fact that the fronts have finite widths (*e.g.*, fig. 2(c)). This is a robust feature of the system; the widths develop quickly after the rake begins to move and remain stable over time. Phenomenologically, this can be accounted for by the inclusion of a diffusive term in eq. (4), which results in the viscous Burgers equation given by

$$U_t + \left(U v_r \left(U + \frac{\phi_0}{\phi_j - \phi_0} \right) \right)_x = D U_{xx}, \qquad (6)$$

where D is a diffusion coefficient (note that eq. (1) is a solution). Equation (6) predicts that the width of the front is given by $\Delta_f = D/v_r$. In principle, the right hand side of eq. (6) could be related either to viscous behavior, *i.e.* diffusion of momentum, or to the physical diffusion of particles. Dimensionally, D, which has units of length over time squared, can be interpreted as the product of a

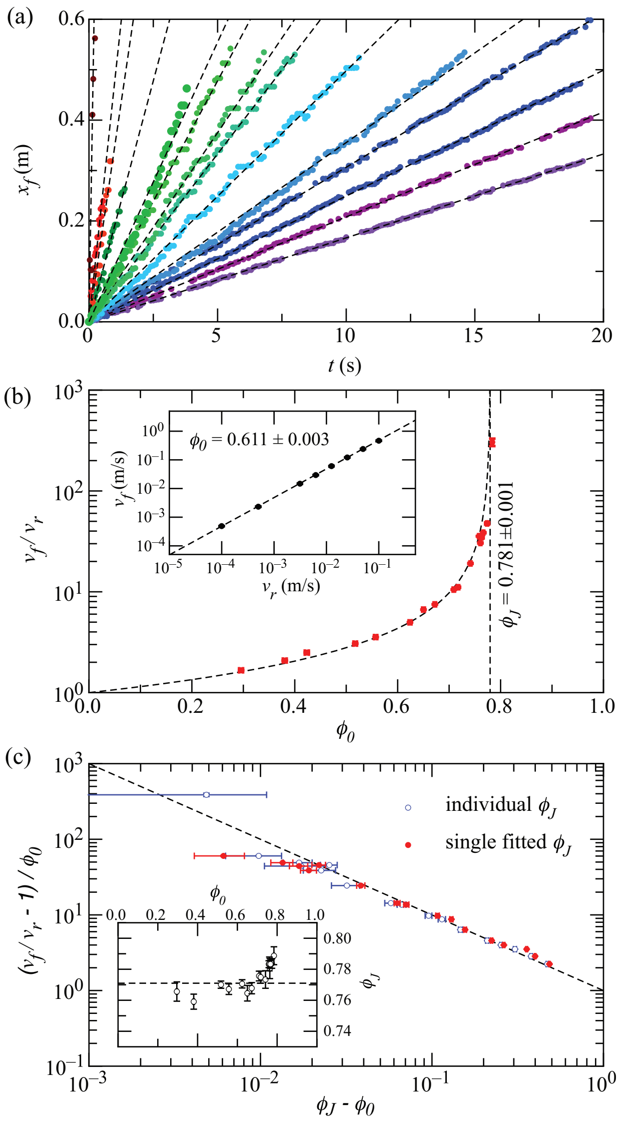

Fig. 3: (Color online) Jamming front dynamics. (a) Front trajectories x_f *vs.* t for $v_r = 1.00 \times 10^{-2}$ m/s and with initial packing fractions (bottom to top) ϕ_0=0.296, 0.381, 0.423, 0.517, 0.557, 0.624, 0.650, 0.672, 0.694, 0.717, 0.741, 0.763, 0.774, 0.784. (b) Ratio of front velocity to rake velocity v_f/v_r *vs.* ϕ_0. The dashed line is a fit to eq. (5) with fit parameter $\phi_J = 0.781 \pm 0.001$. Inset: v_f *vs.* v_r shows $v_f \propto v_r$ at fixed $\phi_0 = 0.611 \pm 0.003$. (c) Rescaled version of (b) using single ϕ_J value calculated from fit (closed red circles) and individual ϕ_J values measured from each experiment (open blue circles). The dashed line is a prediction based on eq. (5) (not a fit). Inset: plot of ϕ_J *vs.* ϕ_0 shows slight increasing trend.

characteristic velocity and lengthscale. The only velocity scale in our system is the speed of the rake. As we have already shown in fig. 2(a), v_r directly affects the front speed. In fig. 4(a) we demonstrate that v_r also sets the scale of the velocity fluctuations δV, which we take to be time-averaged, standard deviation of the disk velocities in the x-bin nearest to the front center (see also the inset to fig. 4(a), which shows the fluctuations are *insensitive* to $\phi_J - \phi_0$). First guesses for the lengthscale might include the disk diameter, the tray width, or the mean free path. However, as we show in fig. 4(b), the width of the front dramatically *increases* as the system density is increased, while these lengthscales remain constant or approach zero.

On the other hand, the appearance of a divergent lengthscale on approach to ϕ_J has been encountered in many jamming studies. In particular, it has been seen in several simulations of *frictionless*, binary-sized disks with identical size and number ratios to those used here. O'Hern *et al.* showed that the extent of moving disks caused by an infinitesimal disturbance of a probe disk diverges on approach to jamming [5]. Similar results were explored in more detail by Reichhardt and coworkers [17], who studied the lateral extent of moving disks as a probe disk was dragged through with a constant force. More recently, Olsson and Teitel showed that the same-time transverse velocity correlation length for a sheared system of binary disks has similar divergent behavior [16]. In general, the divergent lengthscales encountered exhibit power-law growth, *i.e.* $\xi \propto (\phi_J - \phi_0)^{-\nu}$. The value of ν varies from one study to the next and its precise value is still a topic of great interest. For the above-mentioned simulations that are similar to our experiment [5,16,17], ν has typically been found to be around 0.6 or 0.7 (although Vågberg *et al.* [27] found $\nu \approx 1$ in a similar binary-disk system by considering finite size effects). In the inset to fig. 4(b), we plot the front width Δ_f *vs.* $\phi_J - \phi_0$. The data exhibit deviations from a straight line on the log-log graph, but if we assume they follow a power law, we see they are consistent with an exponent around 0.65, *i.e.* in the same range as the previous studies. This is suggestive that the growing front width we see here may be a signature of the divergent lengthscale seen more generally in jamming systems.

To take this comparison one step further, we measure the equal-time longitudinal velocity correlation function of our system. Symmetry dictates that the only position relative to which we can calculate a meaningful correlation function is at the center of the front (calculating it at positions behind the front will yield a correlation length that grows with time, and beyond it yields zero). We therefore define the correlation length here as

$$\xi = \frac{1}{v_r^2}\left(\int_{-\infty}^{x_f} (v_r - V(x))V(x_f)\mathrm{d}x + \int_{x_f}^{\infty} V(x_f)V(x)\mathrm{d}x\right). \quad (7)$$

We do this calculation on both sides of the front because we find there is a slight tendency for the upstream value to be higher than the downstream value, indicating a slight asymmetry in the front shape. In fig. 4(c), we plot ξ *vs.* Δ_f, which shows that they are indeed related by a simple linear scaling whose slope (~1.6) is close to what would be expected from calculating the same correlation function from eq. (1) ($2\ln(2) \approx 1.4$).

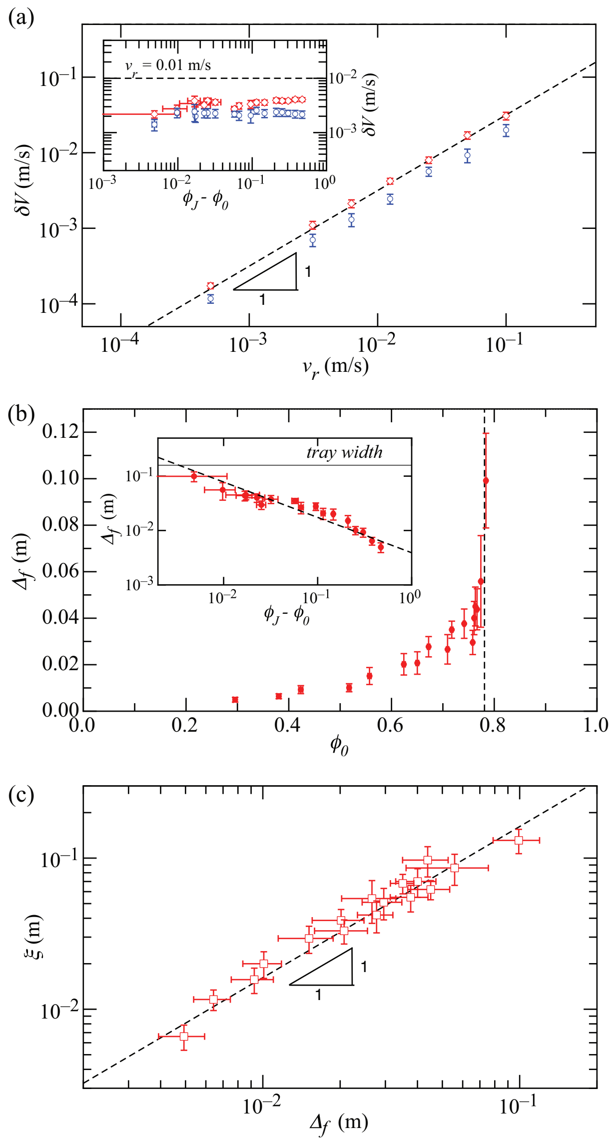

Fig. 4: (Color online) Growing front width and correlation length. (a) Time-averaged longitudinal (red diamonds) and transverse (blue circles) root mean square velocity fluctuations δV at the front center *vs.* rake velocity v_r. Inset: δV shows little dependence on $\phi_J - \phi_0$ (symbols same as (a)). (b) Front width Δ_f *vs.* ϕ_0 shows strong growth, indicating incompatibility with diffusive broadening. Inset: Δ_f *vs.* $\phi_J - \phi_0$ on log-log graph (note that individually measured values of ϕ_J are used). The dashed line is a power law with $\nu = 0.65$ drawn as a guide to the eye (see text). (c) Longitudinal velocity correlation length ξ *vs.* front width Δ_f. The fit is linear with coefficient ∼1.6 and offset 0.

Discussion and conclusions. – In these experiments we focused on the dynamic process by which a jamming front spreads throughout a system. Uniaxially compressing the 2D collection of disks leads to local densification that travels along the compression axis, leaving the regions behind it jammed. The jamming fronts can be characterized by either the velocity or packing fraction profiles, which translate stably over time and exhibit well-defined speeds and widths. Unlike shocks that occur in systems above ϕ_J, the front speeds in this highly damped system are proportional to the driving speed v_r and determined entirely by disk conservation and rigidity onset. However, the well-defined widths of the jamming fronts cannot be explained by disk conservation alone. Instead, we show that the front width can be related to the velocity correlation function, which has been found to diverge near jamming in recent simulations. While the experiments discussed here concerned a 2D system of particles, the description is quite general and we expect similar, well-defined propagating density fronts to occur generically in systems near jamming. In particular, we believe that the fronts recently observed in 3D dense suspensions during impact-activated solidification [13] are triggered by the same phenomenon.

* * *

We thank Sidney Nagel, Martin van Hecke, Wendy Zhang, Marc Miskin, Nitin Upadhyaya and Doug Durian for discussions. We thank the referees for constructive comments that improved the manuscript. This work was supported by the National Science Foundation (NSF) through its Materials Research Science and Engineering program (DMR-0820054). SRW was supported by the U.S. Department of Energy, Office of Basic Energy Sciences, Division of Materials Sciences and Engineering under Award DE-FG02-03ER46088. LKR acknowledges support through the NSF Research Experience for Undergraduates program.

REFERENCES

[1] Liu A. J. and Nagel S. R., *Nature*, **396** (1998) 21.
[2] Zhang Z., Xu N., Chen D. T. N., Yunker P., Alsayed A. M., Aptowicz K. B., Habdas P., Liu A. J., Nagel S. R. and Yodh A. G., *Nature*, **459** (2009) 230.
[3] Majmudar T. S. and Behringer R. P., *Nature*, **435** (2005) 1079.
[4] Bi D., Zhang J., Chakraborty B. and Behringer R. P., *Nature*, **480** (2011) 355.
[5] O'Hern C. S., Silbert L. E., Liu A. J. and Nagel S. R., *Phys. Rev. E*, **68** (2003) 011306.
[6] Keys A. S., Abate A. R., Glotzer S. C. and Durian D. J., *Nat. Phys.*, **3** (2007) 260.
[7] Cheng X., *Phys. Rev. E*, **81** (2010) 031301.
[8] Majmudar T., Sperl M., Luding S. and Behringer R., *Phys. Rev. Lett.*, **98** (2007) 058001.
[9] Liu A. J. and Nagel S. R., *Annu. Rev. Condens. Matter Phys.*, **1** (2010) 347.
[10] To K., Lai P.-Y. and Pak H., *Phys. Rev. Lett.*, **86** (2001) 71.
[11] Sheldon H. G. and Durian D. J., *Granular Matter*, **12** (2010) 579.
[12] Davis R. H. and Acrivos A., *Annu. Rev. Fluid Mech.*, **17** (1985) 91.
[13] Waitukaitis S. R. and Jaeger H. M., *Nature*, **487** (2012) 205.

[14] Shundyak K., Van Hecke M. and Van Saarloos W., *Phys. Rev. E*, **75** (2007) 010301.
[15] Papanikolaou S., O'Hern C. S. and Shattuck M. D., arXiv:1207.6010 [cond-mat.soft] (2012).
[16] Olsson P. and Teitel S., *Phys. Rev. Lett.*, **99** (2007) 178001.
[17] Olson Reichhardt C. J. and Reichhardt C., *Phys. Rev. E*, **82** (2010) 051306.
[18] Drocco J., Hastings M., Reichhardt C. and Reichhardt C., *Phys. Rev. Lett.*, **95** (2005) 088001.
[19] Schneider C. A., Rasband W. S. and Eliceiri K. W., *Nat. Methods*, **9** (2012) 671.
[20] Crocker J. C. and Grier D. G., *J. Colloid Interface Sci.*, **179** (1996) 298.
[21] Rycroft C. H., *Chaos*, **19** (2009) 041111.
[22] Beatus T., Tlusty T. and Bar-Ziv R., *Phys. Rev. Lett.*, **103** (2009) 114502.
[23] Ellenbroek W. G., Zeravcic Z., van Saarloos W. and van Hecke M., *EPL*, **87** (2009) 34004.
[24] Courant R. and Friedrichs K. O., *Supersonic Flow and Shock Waves* (Springer, Berlin) 1985.
[25] Gómez L., Turner A., Van Hecke M. and Vitelli V., *Phys. Rev. Lett.*, **108** (2012) 058001.
[26] Gómez L., Turner A. and Vitelli V., *Phys. Rev. E*, **86** (2012) 041302.
[27] Vågberg D., Valdez-Balderas D., Moore M. A., Olsson P., and Teitel S., *Phys. Rev. E*, **83** (2011) 010301.